

# Fluorescence-Based Assessment of Plasma-Induced Hydrophilicity in Microfluidic Devices via Nile Red Adsorption and Depletion

David J. Guckenberger,<sup>†</sup> Erwin Berthier,<sup>†,‡</sup> Edmond W. K. Young,<sup>§</sup> and David J. Beebe<sup>\*,†</sup>

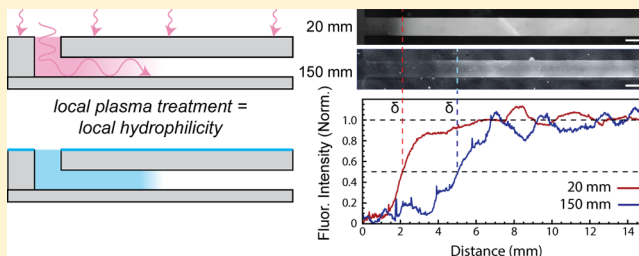
<sup>†</sup>Department of Biomedical Engineering, Wisconsin Institutes for Medical Research, University of Wisconsin-Madison, 1111 Highland Avenue, Madison, Wisconsin 53705, United States

<sup>‡</sup>Department of Medical Microbiology, University of Wisconsin-Madison, 1550 Linden Drive, Madison, Wisconsin 53706, United States

<sup>§</sup>Department of Mechanical & Industrial Engineering, Institute of Biomaterials and Biomedical Engineering, University of Toronto, 5 King's College Road, Toronto, Ontario M5S 3G8 Canada

## S Supporting Information

**ABSTRACT:** We present a simple method, called fluorescence-based assessment of plasma-induced hydrophilicity (FAPH), that enables spatial mapping of the local hydrophilicity of surfaces normally inaccessible by traditional contact angle measurement techniques. The method leverages the change in fluorescence of a dye, Nile Red, which is adsorbed on an oxygen plasma-treated surface, and its correlation with the contact angle of water. Using FAPH, we explored the effect of microchannel geometries on the penetration distance of oxygen plasma into a microchannel and found that entrance effects prevent uniform treatment. We showed that these variations have a significant impact on cell culture, and thus the design of cell-based microfluidic assays must consider this phenomenon to obtain repeatable and homogeneous results.



Hydrophilicity, or wettability, is an important physical property of microfluidic systems, especially regarding its internal surfaces. Many microfluidic systems rely on surface hydrophilicity to achieve various functions such as (i) facilitating capillary fluid flow into microchannels (i.e., priming);<sup>1</sup> (ii) preventing nonspecific hydrophobic adsorption of sample molecules;<sup>2,3</sup> and (iii) promoting attachment of mammalian cells in tissue culture for cell-based applications.<sup>4,5</sup> For microfluidic systems fabricated in glass, the internal surfaces are naturally hydrophilic and thus do not require additional treatment to achieve the above functions. However, for microfluidic systems fabricated in other commonly used materials such as poly(dimethylsiloxane) (PDMS),<sup>6</sup> polystyrene (PS),<sup>7</sup> and cyclo-olefin copolymers (COC),<sup>8,9</sup> the internal surfaces are naturally hydrophobic and require surface modification to render them hydrophilic. Because these materials are becoming increasingly popular for the development of microfluidic systems,<sup>10,11</sup> the ability to not only render these materials hydrophilic but to also retain and characterize their hydrophilicity are crucial to advancing microfluidics technology and expanding its applications.

A common method of achieving hydrophilicity is to expose surfaces to oxygen plasma. Plasma treatments are used in many applications including the removal of organic contaminants,<sup>12,13</sup> the control of surface wettability,<sup>14</sup> and the traditional application of making plastic substrates hydrophilic to facilitate cell adhesion and growth in laboratory plasticware (e.g., polystyrene Petri dishes and well plates).<sup>15</sup> In addition, oxygen

plasma treatments activate surfaces to enable bonding between two interfaces<sup>16</sup> and have been widely employed in the microfluidics community to bond PDMS to glass (or other materials) to create enclosed microchannels.<sup>17</sup> The convenience and accessibility of plasma treatment allows it to be incorporated into laboratory procedures without the need for dry or wet chemical processes.

Although achieving hydrophilicity is straightforward, the ability to retain hydrophilicity is dependent on the material. PS retains its hydrophilicity, allowing commercial plasticware to have long shelf lives (i.e., years). PDMS, conversely, is known to undergo hydrophobic recovery in a matter of hours.<sup>18</sup> This often imposes a time constraint on experimental procedures, adds variability to test conditions, and constitutes one of several important factors that has hindered widespread adoption and commercialization of PDMS-based microfluidic systems. Because of the steady convergence of microfluidics and cell biology applications and the ongoing pursuit of commercial, user-friendly microfluidic technologies (including tools for point-of-care diagnostics<sup>19</sup> and platforms for microfluidic cell culture<sup>7</sup>), there is a clear need to develop microfluidic systems made of common manufacturable materials like PS and COC that have potential for high volume industrial production and can maintain stable surface characteristics such as hydro-

Received: April 7, 2014

Accepted: July 4, 2014

Published: July 4, 2014

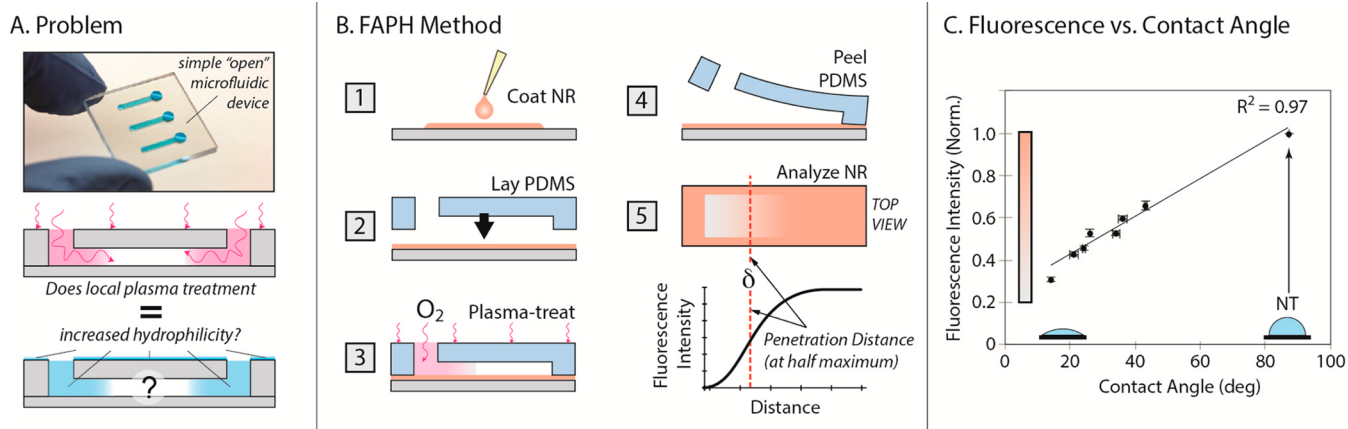


**Figure 1.** (A) Plasma treatment before device assembly can adversely affect bond quality. While it is advantageous to plasma-treat after bonding, the effectiveness of the treatment within the channel is unknown. (B) The FAPH method: (1) apply the NR coating, (2) assemble microchannels, (3) plasma treat, (4) remove microchannels, and analyze fluorescence. Penetration distance,  $\delta$ , is determined by finding the half-maximum of fluorescence intensity. (C) Relationship between contact angle and fluorescence intensity, normalized to maximum intensity (untreated PS).

philicity.<sup>10</sup> Thus, researchers have been studying and developing methods to facilitate the testing and characterization of robust, surface-treated plastic microfluidic devices in the lab, in hopes of eventually translating these techniques to industry.<sup>3,7,10,20–24</sup>

Two current challenges in fabricating robust plastic microfluidic devices are (i) the ability to apply uniform plasma treatments within the entire device and (ii) the ability to characterize the surface hydrophilicity after treatment to assess its uniformity. In the case of PDMS-PDMS and hybrid PDMS-glass microfluidic devices, plasma treatments are typically applied prior to device assembly because it simultaneously activates the surfaces for bonding and uniformly hydrophilizes all internal surfaces. However, in the case of thermoplastic microfluidic devices, oxygen plasma treatment prior to thermal diffusive bonding tends to reduce bond strength,<sup>7</sup> making plasma treatment before device bonding undesirable. Applying plasma treatment after bonding is plausible,<sup>23</sup> particularly for microfluidic devices that employ open access ports,<sup>25</sup> but because the plasma is entering only through the access ports, the treatment may not be uniform within the device and penetration into microchannels may be limited (Figure 1A).<sup>26,27</sup> Further research is therefore necessary to advance our ability to generate and retain uniform hydrophilic surfaces via plasma treatment in plastic microfluidic devices. In addition, improved methods that characterize the uniformity of plasma treatment and correlate it to surface hydrophilicity are needed. While measuring contact angles of droplets is the most common method for assessing wettability,<sup>28</sup> it relies on the use of relatively large (microliter) droplets that are not suitable for assessing local wettability at high spatial resolution.

Here, we describe a novel approach called fluorescence-based assessment of plasma-induced hydrophilicity (FAPH) that is suitable for characterizing local surface wettability at high spatial resolution (Figure 1B). The approach relies on adsorption of a hydrophobic, fluorogenic molecule, Nile Red (NR), on the substrate surface, subsequent plasma treatment to deplete NR molecules, and fluorescence image analysis to quantify the level of NR depletion and determine the *in situ* surface hydrophilicity. The purpose of FAPH is to provide microfluidic designers with insight on microscale geometries and physical dimensions that account for how plasma treatment modifies

surface hydrophilicity. By applying this approach, we explored the effects of geometry on plasma treatment penetration and, as a demonstration of its importance in future cell-based applications, studied the downstream effects of the applied plasma treatment on the adhesion of mammalian cells in microscale cell culture.

## METHODS AND MATERIALS

**Microchannel Fabrication.** Microchannels were fabricated in PDMS using established soft lithography techniques.<sup>6,17</sup> A master mold was fabricated by spin-coating photoresist (SU-8 100, Microchem, Newton, MA) onto a silicon wafer (WRS Materials, San Jose, CA) and patterning the channel features using UV light (Omnicure series-1000, EXFO, Mississauga, Canada). Unexposed photoresist was removed with SU-8 developer (PG-MEA no. 484431, Sigma-Aldrich, St. Louis, MO). Features were molded by soft lithography using PDMS (Sylgard 184, Dow Corning, Midland, MI) mixed in a 10:1 ratio of elastomer base and curing agent and baked on a hot plate at 80 °C for 4 h. Channels varied in height from 100 to 350  $\mu\text{m}$  and in width from 0.10 to 1.0 mm. PDMS microchannels were then passively bonded to PS substrates for subsequent tests.

**PS Sample Preparation.** Samples were fabricated in 1.2 mm thick PS sheets (no. ST313120, Goodfellow, Huntingdon, England). Large (60 mm  $\times$  90 mm) and small (25 mm  $\times$  25 mm) samples pieces were cut using a Personal CNC Mill (PCNC 770, Tormach, Waunakee, WI). Samples were cleaned by rinsing with deionized (DI) water, sonicating for 15 min in 50 °C isopropyl alcohol (IPA), and rinsing again by submerging in a DI water bath for 1 min. Cleaned samples were pulled out of the DI water bath slowly to ensure that the surface was free from any satellite water droplets. Nile Red (NR) (no. N3013, Sigma-Aldrich) was diluted to 5  $\mu\text{g/mL}$  in DMSO (no. D2650, Sigma-Aldrich) to obtain a stock solution, and then further diluted 1:200 (v/v) in IPA to yield the working solution. The working NR solution was applied on one side of the PS sample at  $\sim 0.35 \mu\text{L/mm}^2$  using a micropipet and left on the surface for 30 s. The sample was then promptly placed in DI water and rinsed as previously described. During rinsing, it was important to remove all satellite water droplets because they tended to leave dried spots on the surface that affected image analysis.

After rinsing, NR-coated samples were protected from light and dust until ready for use.

**Plasma Treatment.** NR-coated PS samples were either assembled to create enclosed microchannels or left unbonded to expose the entire sample. Samples were treated with oxygen plasma using a plasma cleaning system (Femto, Diener Electronic, Ebhausen, Germany). Plasma treatments varied in exposure time (5–50 s), oxygen gas flow rate (20–40 mL/min), and power (25–50 W), which were chosen based on previously published work.<sup>7,23,25</sup> Unbonded PS samples were used to obtain a correlation between NR fluorescence intensity and contact angle measurements made via standard goniometry of sessile drops (see Contact Angle Measurements). Assembled PS samples, with the passively bonded microchannels, were used for characterizing plasma treatment penetration into microchannels by fluorescence quantification. In these experiments, PDMS microchannels were passively bonded to the NR-coated samples, plasma treatment was applied into the channels, and the PDMS microchannels were then removed after plasma treatment, exposing the entire sample surface to image analysis. Plasma treatments in these experiments were applied consistently for 50 s, at 50 W, and with an oxygen gas flow rate of 20 mL/min.

**Contact Angle Measurements.** Surface hydrophilicity of PS samples was characterized by measuring and averaging contact angles of three 6  $\mu$ L DI water droplets on the sample surface using a goniometer (model 200, Ramé-Hart, Succasunna, NJ). For all PS samples that were NR-coated and imaged for fluorescence, fluorescence imaging was always performed prior to contact angle measurements, to prevent potential disruption of the homogeneous NR coating via the 6- $\mu$ L DI water droplets.

**Fluorescence Imaging and Analysis.** All NR-coated samples were imaged on an inverted fluorescence microscope (Eclipse Ti, Nikon) using appropriate filters. Images of NR-coated samples were acquired both before and after plasma treatment to enable assessment of the depletion of NR fluorescence caused by plasma treatment. To obtain a correlation between NR fluorescence intensity and contact angle, each NR-coated PS sample was imaged at nine locations, which were averaged to represent the fluorescence intensity for that PS sample (three samples per treatment condition). To spatially “map” fluorescence within microchannels, images were flatfield-corrected using ImageJ and stitched using Adobe Photoshop. To quantify penetration distance of plasma treatment, the fluorescence intensity along the channel length was averaged across the channel width. The resulting intensity profile was analyzed to determine the location where the intensity reached half of its maximum, and this location was then defined as the penetration distance,  $\delta$  (Figure 2).

**Cell Culture, Imaging, and Analysis.** See the Supporting Information for details on cell culture, imaging, and analysis.

## RESULTS

**Overview.** We developed a method called fluorescence-based assessment of plasma-induced hydrophilicity (FAPH) that allows characterization of local surface hydrophilicity of internal surfaces within microchannels (Figure 1B) and informs how microfluidic geometries and dimensions can impact the effectiveness of plasma treatment. The methodology relies on the following steps: (1) uniform coating of sample with NR, a hydrophobic fluorescent dye that adsorbs to hydrophobic surfaces because of hydrophobic interactions; (2) passive

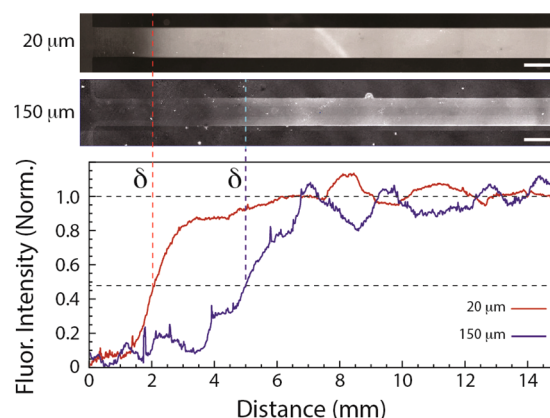


**Figure 2.** Penetration distance,  $\delta$ , is determined by finding the half-maximum of the fluorescent intensity along the channel length. The representative stitched fluorescence maps of 800- $\mu$ m microchannels are shown for 20- $\mu$ m (top image) and 150- $\mu$ m (bottom image) tall microchannels. The fluorescence intensity profiles (averaged across channel width) are normalized to the maximum intensity of each channel, determined by averaging the intensity of the last 4 mm of the channel length (scale bars represent 1 mm).

(reversible) assembly of PDMS microchannels onto the NR-coated sample; (3) treatment with plasma under desired parameters; (4) removal of PDMS microchannels to expose the plasma-treated substrate; and (5) fluorescence quantification of NR over the entire microchannel pattern, and correlation to surface hydrophilicity via contact angle calibration.

FAPH relies on the observation that upon plasma treatment, adsorbed NR on a surface undergoes a decrease in fluorescence intensity, or a fluorescence depletion, correlated to the level of plasma applied. An important aspect of the method is the need to establish a uniform NR coating. We accomplished this by dissolving NR in IPA, which leveraged IPA's low surface tension and its inherent property of enhancing NR fluorescence.<sup>29</sup> We found the optimal adsorption time for NR to range between 15 and 30 s, which allowed the dye to quench,<sup>30</sup> yielding a dimmer but more homogeneous and repeatable NR coating with adequate fluorescence (Figure S1 in the Supporting Information). We thus chose a 30 s adsorption time for all experiments. When protected from light, external contaminants, and extraneous contact, NR-adsorbed PS samples were found to be stable for several weeks and could be safely stored for weeks before experimentation.

**NR Fluorescence Intensity vs Contact Angle Correlation.** To use NR fluorescence as a quantitative indicator of hydrophilicity, we correlated NR fluorescence to contact angle measurements, the standard for characterizing surface wettability. Contact angles were measured, both before and after plasma treatment, via goniometry with water droplets placed on NR-adsorbed PS samples. Adsorbed NR itself did not significantly affect the contact angle measurement, as evidenced by negligible differences between NR-adsorbed and non-NR-adsorbed samples (Figure S2 in the Supporting Information). Plasma treatment was controlled by tuning the power, flow rate, and exposure time. We found a linear relationship between NR fluorescence intensity and contact angle (Figure 1C) for angles between 15° and 50°. We were unable to obtain contact angles between ~50° and 85° (note, 85° was the contact angle of untreated PS), because the most gentle plasma treatment applied (i.e., lowest power setting, highest pressure setting, and shortest duration) resulted in a decrease in contact angle to



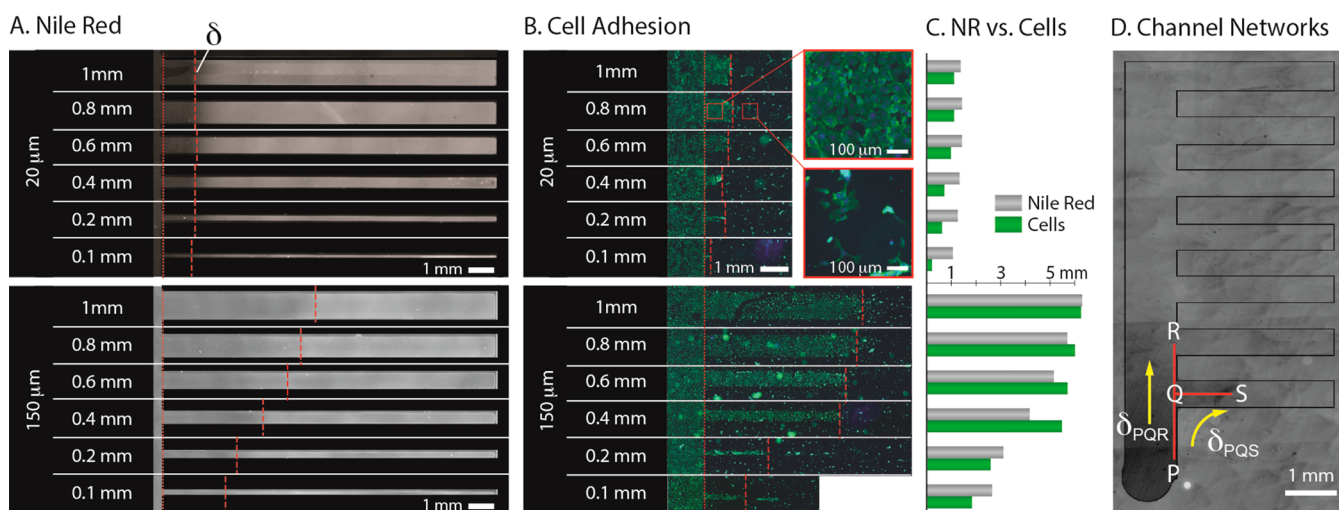


**Figure 3.** (A) Stacked fluorescence maps of plasma-treated NR coatings in 20 and 150  $\mu\text{m}$  tall channels. (B) HUVECs cultured on plasma-treated surface after microchannel removal. Insets show HUVEC morphology in hydrophilic and hydrophobic regions of channel (green = f-actin stained via phalloidin; blue = nuclei stained via Hoechst dye). In parts A and B, dotted red line = entrance; dashed red line =  $\delta$ . (C) Graph comparing measured  $\delta$  in parts A and B. (D) Stacked fluorescence map of a microchannel network. Red lines indicate  $\delta$  measured as a straight line path from inlet port P.  $\delta_{PQR} = 2.24$  mm and  $\delta_{PQS} = 2.38$  mm.

$\sim 50^\circ$ . We were also unable to obtain measurements of contact angles  $< 15^\circ$  because all angles less than  $15^\circ$  could not be distinguished from  $0^\circ$  by goniometry and were thus considered highly hydrophilic. Nevertheless, our results yielded two important observations: (1) fluorescence intensity is linearly correlated to contact angle, and (2) fluorescence intensity can be used to inform us of the contact angle, and thus the surface hydrophilicity. Importantly this information is independent of the plasma treatment parameters used to achieve the contact angle. If two different sets of treatment parameters achieved the same contact angle (e.g., high power over short exposure time versus low power over long exposure time), then the resultant fluorescence intensity would be the same. This result confirmed that NR fluorescence intensity can be used as an indirect metric for contact angle and, by extension, the hydrophilicity of internal microchannel surfaces.

**NR Microchannel Characterization.** The linear correlation between NR fluorescence intensity and contact angle allowed us to employ the FAPH method to assess surface hydrophilicity after plasma treatment within microchannel geometries. To assess the effect of geometry and entrance effects on the penetration of plasma treatment into microchannels, we fabricated microchannels with different heights (20, 150, and 350  $\mu\text{m}$ ) and widths (0.1–1 mm, Figure 3A and Figure S3 in the Supporting Information). The microchannels were open on only one end (left, entrance indicated by dotted red line) to allow unidirectional plasma penetration and were all treated under the same parameters (see the Methods and Materials). We observed a visible decrease in NR fluorescence intensity beginning at the channel entrance and extending into the channel for a specific distance (solid red line path), followed by transition back to the original level of NR fluorescence intensity. On the basis of our observations that NR fluorescence intensity is linearly correlated with contact angle (Figure 1C) and specific contact angles are correlated to applied plasma treatment, the observed intensity decrease was attributed to local oxygen plasma exposure that depleted the adsorbed NR.

We defined the plasma treatment penetration distance,  $\delta$ , as the distance from the entrance to the location where the NR fluorescence intensity returns to 50% of the original NR level. On the basis of this definition and the curve fit between fluorescence intensity and contact angle (Figure 1C),  $\delta$  represented a contact angle of  $\sim 28^\circ$ , considered moderately hydrophilic.  $\delta$  was then compared across different microchannel cross-sectional dimensions (Figures 2 and 3A). First, we found that  $\delta$  was influenced most by microchannel height. For 20  $\mu\text{m}$  tall channels,  $\delta$  ranged from  $\sim 1$  to  $\sim 1.4$  mm, while for 150  $\mu\text{m}$  tall channels,  $\delta$  reached 5.5 mm. Second, we found that channel width had little impact for 20  $\mu\text{m}$  tall channels but had significantly more impact for 150  $\mu\text{m}$  tall channels. For 20  $\mu\text{m}$  tall channels,  $\delta$  consistently reached  $\sim 1$  mm for widths ranging from 0.1 to 1.0 mm. In contrast, for 150  $\mu\text{m}$  tall channels,  $\delta$  reached 3 mm into a 0.1 mm wide channel and 5.5 mm into a 1 mm wide channel. We note that microchannels as tall as 350  $\mu\text{m}$  were tested (Figure S3 in the Supporting Information), but these results displayed high variability, suggesting that plasma treatment became less uniform for taller channels. Overall, the results showed importantly that  $\delta$  depended on microchannel cross-sectional dimensions. Furthermore, the results demonstrated the utility of FAPH to enable visualization of plasma treatment levels and led to local “spatial mapping” of surface hydrophilicity. The acquired spatial maps indicated a hydrophilicity gradient from the entrance inward.

**Microchannel Cell Characterization.** After visualizing spatial maps of surface hydrophilicity and measuring  $\delta$  in microchannels, we investigated the impact of the observed hydrophilicity gradient on cell culture (Figure 3B). We hypothesized that cell adhesion and spread in the microchannels would vary depending on a gradient of surface hydrophilicity and that this gradient would lead to a similar gradient in cell adhesion, i.e., more adherent cells would be near the more hydrophilic entrance region and fewer adherent cells would be seen further into the microchannel. We used the same microchannel design and plasma treatment parameters as for the NR microchannel characterization above but used non-NR-adsorbed PS samples to avoid unnecessary interaction with

cells. After plasma treatment, channels were removed and the sample was submerged in a suspension of human umbilical vein endothelial cells (HUVECs) for 24 h to allow homogeneous and geometry-independent cell seeding (Figure 3B). HUVECs were chosen because they are known to demonstrate a noticeable difference in adhesion and spread when cultured on hydrophobic versus hydrophilic surfaces (Figure S4 in the Supporting Information). We measured the distance from the channel entrance to the point at which cell adhesion was half as high as in the treated area (Figure 3B) and compared this to  $\delta$  obtained by NR depletion. As hypothesized, we observed cells adhering more to the hydrophilic regions compared to hydrophobic regions. Adhesion correlated with penetration distance  $\delta$  and similar trends were observed for both 150 and 20  $\mu\text{m}$  tall channels, with results matching more closely for the taller channels ( $R^2 = 0.95$ ) than for the shorter channels ( $R^2 = 0.77$ ) (Figure 3C and Figure S5 in the Supporting Information).

**FAPH in Microchannel Networks.** Finally, we applied FAPH to a multichannel network consisting of multiple 500  $\mu\text{m}$  wide horizontal microchannels extending from a main 1 mm wide vertical microchannel (Figure 3D). Such a configuration mimics the design for a cell culture microchannel connected to perpendicular conduits, which may then be attached to adjacent cell culture compartments (not shown). We were interested in visualizing the effect of oxygen plasma treatment into an open port (P) and through this configuration. When we analyzed  $\delta$  in the vertical main channel, we found  $\delta_{\text{PQR}} = 2.24$  mm, which did not reach the entrance of the second horizontal arm. When we subsequently analyzed  $\delta$  in all the horizontal arms, only the channel closest to the inlet port showed detectable NR depletion, with  $\delta_{\text{PQS}} = 2.38$  mm. This total straight-line path measured from the inlet port P to location S (Figure 3D) was  $\sim 6\%$  longer than the straight-line path from P to R, indicating a consistency in the penetration distance due to plasma treatment, independent of the tortuosity of the path. Collectively, these results show the importance of homogeneity of plasma treatment in microchannels, and the potential of FAPH for characterizing plasma treatment in simple and complex channel designs

## DISCUSSION

To our knowledge, FAPH is the first fluorescence-based approach for characterizing the internal surface hydrophilicity of microchannels. The main advantage of FAPH is its ability to provide quantitation of the local surface hydrophilicity in a manner that cannot be obtained by conventional methods such as goniometry. Goniometry is effective and efficient for large planar substrates where droplets can be placed on a flat surface and imaged to determine contact angles. Enclosed microchannels, however, are not accessible to contact angle measurements via goniometry because they are not open to sessile drop formation. Furthermore, contact angle measurements only provide a measure of the surface hydrophilicity over areas that cover the footprint of the droplet or larger, so spatial resolution is limited. FAPH is applicable for simple and complex channel designs and configurations (Figure 3D) and is useful for assessing plasma treatments in enclosed microchannels quantitatively in terms of penetration distance  $\delta$ .  $\delta$  was found to correlate closely in cell culture systems with the channel location delineating regions of high and low cell adhesion (Figure 3B) and was found to be dependent on channel dimensions (Figure 3C). Specifically,  $\delta$  appeared to

decrease with decreasing channel width for deep (150- $\mu\text{m}$  tall) channels but was found to be so short for shallow (20 mm tall) channels that decreasing channel width had no additional effect on  $\delta$ . It was also discovered that  $\delta$  was similar in length for different tortuous paths in a complex microchannel network after plasma treatment through a single inlet port (Figure 3D). These geometric effects on plasma treatment are important in cases where microdevices are treated after assembly, which is commonly done for microdevices fabricated in PS because plasma treatment before assembly can adversely affect bonding procedures.<sup>7</sup> FAPH enables characterization of the quality of local plasma treatment in the microchannel network with unparalleled spatial resolution. The technique offers a convenient visual readout via fluorescence that spatially “maps” the surface hydrophilicity, which is impossible with goniometry. This visual information can then be used to inform the user about heterogeneities in wettability and guide optimization. Depending on the biological or fluidic requirements of a microchannel, the designer could choose to use the appropriate microchannel height to ensure homogeneous surface treatment in the channel. For example, if a total channel length of 10 mm is desired, a microchannel that is 1 mm wide and 150  $\mu\text{m}$  tall will ensure plasma penetration of at least 5 mm from one port. Adding a second port at the other end of the microchannel will therefore ensure complete plasma treatment into the center due to penetration from both ends.  $\delta$  was found to be independent of the quantity of access ports and simply dependent on channel geometry (see the Supporting Information).

FAPH currently works best when NR is precoated on the substrate prior to device assembly because it ensures uniform NR adsorption on the surface. The method also yields more consistent fluorescence quantification when the device is disassembled after plasma treatment and before image analysis. We currently achieve this by using a passively bonded PDMS channel layer that can be removed after plasma treatment. This was sufficient to model the effects of channel dimensions on plasma treatment effectiveness, since it was found during preliminary testing that the PDMS, instead of PS, did not change the resultant measurements of  $\delta$ . Future work will investigate how to extend the FAPH method to work directly in enclosed, fully assembled microchannels without the need for precoating of substrates or the need for device disassembly.

In terms of the choice to use NR, we tried other fluorophores (e.g., Texas Red) and found NR to offer the most sensitive detection and yield the most repeatable results. NR sensitivity was further improved by dissolving NR in IPA, which offered increased fluorescence intensity while also improving surface coverage during the dye adsorption step because of the low surface tension of IPA. NR emission wavelengths can be adjusted by changing the solvent,<sup>29</sup> so further optimization can be achieved for other applications if necessary.

The underlying physics of plasma treatment continues to be an active area of research.<sup>31</sup> FAPH has potential to uncover answers to previous questions related to the mechanisms of plasma treatment, particularly in its penetration and effectiveness in complex geometries and configurations. In addition, there may be potential applications where nonuniform plasma treatment is an advantage. In such cases, FAPH will provide a quantitative method for optimizing designs to provide the desired surface treatment, and to assist with the visual “mapping” of surface hydrophilicity.

## CONCLUSION

FAPH is a method for characterizing and mapping the local plasma treatment within microchannels. Our data suggests that NR fluorescence can be directly correlated to contact angle and by extension plasma treatment penetration. Microchannel cross-sectional shape appears to have a significant effect on plasma treatment penetration distance. Channel design therefore plays a critical role in plasma treatment quality. Using this method, channels can be characterized prior to cell culture, thereby aiding device design and reducing the time needed to develop and optimize a functional cell-based assay.

## ASSOCIATED CONTENT

### Supporting Information

Cell culture methods and analysis, motivation for the method based on cell adhesion, data on NR quenching, the impacts NR on contact angle, 350  $\mu\text{m}$  tall microchannels, effects of hydrophilicity on cell adhesion, and a comparison between NR characterization of  $\delta$  and cell culture results. This material is available free of charge via the Internet at <http://pubs.acs.org>.

## AUTHOR INFORMATION

### Corresponding Author

\*E-mail: [djbeebe@wisc.edu](mailto:djbeebe@wisc.edu).

### Notes

The authors declare the following competing financial interest(s): D.J. Beebe has ownership in BellBrook Labs, which licenses part of the technology demonstrated in this manuscript.

## ACKNOWLEDGMENTS

The authors thank both the Nancy Keller lab and the University of Wisconsin Carbone Cancer Center for use of their microscopes. We thank Professor Leon Shohet for his advice of the plasma phenomena. This work was funded by the Bill and Melinda Gates Foundation through a Grand Challenges in Global Health Initiative Grant OPP1028788, National Institutes of Health Grants R01 EB010039 and R01 CA155192, and National Science Foundation Project EFR-1136903.

## REFERENCES

- (1) Zhou, J.; Ellis, A.; Voelcker, N. H. *Electrophoresis* **2010**, *31*, 2–16.
- (2) Vogler, E. *Adv. Colloid Interface* **1998**, *74*, 69–117.
- (3) Van Midwoud, P. M.; Janse, A.; Merema, M. T.; Groothuis, G. M. M.; Verpoorte, E. *Anal. Chem.* **2012**, *84*, 3938–3944.
- (4) Dowling, D. P.; Miller, I. S.; Ardhaou, M.; Gallagher, W. M. *J. Biomater. Appl.* **2011**, *26*, 327–347.
- (5) Yang, S. Y.; Kim, E.; Jeon, G.; Choi, K. Y.; Kim, J. K. *Materials Science and Engineering* **2013**, *33*, 1689–1695.
- (6) Jo, B.; Van Lerberghe, L.; Motsegood, K. M.; Beebe, D. J. *J. Microelectromech. S.* **2000**, *9*, 76–81.
- (7) Young, E. W. K.; Berthier, E.; Guckenberger, D. J.; Sackmann, E.; Lamers, C.; Meyvantsson, I.; Huttenlocher, A.; Beebe, D. J. *Anal. Chem.* **2011**, *83*, 1408–1417.
- (8) Mair, D. A.; Geiger, E.; Pisano, A. P.; Frechet, J. M.; Svec, F. *Lab Chip* **2006**, *6*, 1346–1354.
- (9) Jena, R.; Yue, C.; Lam, Y. *Microsystem tech.* **2012**, *2*, 159–166.
- (10) Berthier, E.; Young, E. W. K.; Beebe, D. J. *Lab Chip* **2012**, *12*, 1224–1237.
- (11) Sackmann, E. K.; Fulton, A. L.; Beebe, D. J. *Nature* **2014**, *507*, 181–189.
- (12) Lee, C.; Kim, H. W.; Kim, S. *Appl. Surf. Sci.* **2007**, *253*, 3658–3663.
- (13) Grace, J. M.; Gerenser, L. J. *J. Disper. Sci. Tech* **2003**, *24*, 305–341.
- (14) Guruvanket, S.; Rao, G. M.; Komath, M.; Raichur, A. K. *Appl. Surf. Sci.* **2004**, *236*, 278–284.
- (15) Barker, S. L.; LaRocca, P. J. *Journal of Tissue Culture Methods* **1994**, *16*, 151–153.
- (16) Tang, L.; Lee, N. *Lab Chip* **2010**, *10*, 1274–1280.
- (17) Duffy, D. C.; McDonal, J. C.; Schueller, O. J. A.; Whitesides, G. M. *Anal. Chem.* **1998**, *70* (23), 4974–4984.
- (18) Eddington, D. T.; Puccinelli, J. P.; Beebe, D. J. *Sensor Actuat B-Chem.* **2006**, *114*, 170–172.
- (19) Chin, C. D.; Linder, V.; Sia, S. *Lab Chip* **2012**, *12*, 2118–2134.
- (20) Becker, H.; Gaertner, C. *Anal. Bioanal. Chem.* **2008**, *390*, 89–111.
- (21) Wang, Y.; Balowski, J.; Phillips, C.; Phillips, R.; Sims, C. E.; Allbritton, N. L. *Lab Chip* **2011**, *11*, 3089–3097.
- (22) Su, X.; Young, E. W. K.; Underkofler, H. A. S.; Kamp, T. J.; January, C. T.; Beebe, D. J. *J. Biomol. Screen* **2011**, *16*, 101–111.
- (23) Guckenberger, D. J.; Berthier, E.; Young, E. W. K.; Beebe, D. J. *Lab Chip* **2012**, *12*, 2317–21.
- (24) Young, E. W. K.; Berthier, E.; Beebe, D. J. *Anal. Chem.* **2013**, *85*, 44–49.
- (25) Berthier, E.; Guckenberger, D. J.; Cavar, P.; Huttenlocher, A.; Keller, N. P.; Beebe, D. J. *Lab Chip* **2013**, *13*, 424–431.
- (26) Tan, S. H.; Nguyen, N. T.; Chua, Y. C.; Kang, T. E. *Biomechanics* **2010**, *4*, 032204–1–032204–8.
- (27) Riaz, A.; Gandhiraman, R.; Dimov, I. *Lab Chip* **2012**, *12*, 4877–4883.
- (28) Kwox, D. Y.; Neumann, A. W. *Adv. Colloid Interfac* **1999**, *81*, 167–249.
- (29) Dutta, A.; Kamada, K.; Ohta, K. *J. Photoch. Photobio. A* **1996**, *93*, 57–64.
- (30) Bohnert, J.; Karamian, B.; Nikaido, H. *Antimicrob. Agents Ch* **2010**, *54*, 3770–3775.
- (31) Eden, J. G.; Park, S. J.; Cho, J. H.; Kim, M. H.; Li, B.; Kim, E. S.; Kim, T. L.; Lee, S. K.; Kim, K. S.; Yoon, J. K.; Sung, S. H.; Sun, P. *IEEE Trans. Plasma Sci.* **2013**, *41*, 661–675.